

Gas Holdup in Stacked Expanded Metal Sheets

Stella Piovano and Ursula Böhm

Departamento de Industrias, Universidad de Buenos Aires, Ciudad Universitaria, 1428 Buenos Aires, Argentina

Juan I. Franco

CITEFA-CIC-PRINSO-Zufriategui 4380, 1603 Villa Martelli, Buenos Aires, Argentina

The gas holdup in different arrays of expanded metal sheets was determined by the conductimetric method.

A model had to be developed for analyzing the conductimetric behavior of the cell in the presence of the metallic sheets. The validity of this model has been verified with single phase flow. The application to two-phase flow allowed the obtaining of information on gas accumulation within stacked expanded metal sheets, showing a strong influence of the geometry of the array. Depending on the orientation of the stacked sheets and of the large dimension of the expanded metal, the gas holdup within the packing will be equal or larger than in an empty bubble column.

Introduction

The interest in two-phase gas-liquid systems has grown enormously in recent years, due to the fact that such systems find multiple uses in the process industry. In certain chemical reactors a gaseous dispersion flows through a fixed bed of solid particles, either catalytic or inert, two-phase upward flow (packed bubble-bed reactors) or downward flow (trickle-bed reactors) being used.

In a reactor with cocurrent upflow the gas phase moves in a dispersed flow, while the liquid is the continuous phase. The role of the packing is to avoid back-mixing, to hinder bubble coalescence and to improve heat dissipation. Furthermore, the presence of the packing allows reliable scaling-up to be carried out (Gianetto and Silvestone, 1986).

There are also many electrochemical processes that operate in the presence of gases. In these cases the electrolyte with dispersed gas exhibits a lower effective electrical conductivity than the pure liquid phase; the gas fraction affects the current distribution and the cell potential.

While a high gas fraction is sought in the above mentioned chemical reactors, in electrochemical cells the gas accumulation is not generally desired. Bubbles can be removed by using, for example, electrodes made of perforated plate, wire mesh or expanded metal which act by diverting the gas bubbles.

There are other electrochemical reactors where the gas is injected from the outside of the cell providing a simple and economical way of stirring the electrolyte (Cavatorta and Böhm, 1987; Cavatorta et al., 1991). A remarkable improvement in

the heat- and mass-transfer phenomena is thus accomplished. In a recent work (Piovano et al., 1988) it has been found that the introduction of expanded metal electrodes (instead of flat plate electrodes), combined with the gas injection, makes it possible to increase the transfer rate by more than 100%.

This fact could be exploited, for example, in the electrochemical absorption used to decontaminate gas streams (Kreysa and Külp, 1983). Owing to the low concentration of the electrochemically active contaminants, three-dimensional electrodes are used. Expanded metal is a suitable material for such electrodes.

If a gas phase is present, either when the expanded metal is a catalyst (or catalyst support) in a chemical reactor or an electrode in an electrochemical reactor, the gas holdup will be an important design parameter and will depend on geometric characteristics of the packed bed as much as on the flow velocities.

One way to determine the gas holdup is through electrical conductivity measurements in the gas-liquid system.

The relation of the electrical conductance of a two-phase dispersion to the conductances of the pure phases has been the subject of numerous theoretical and empirical investigations, as reviewed by Meredith and Tobias (1962) and by Vogt (1983). Among the various equations available in literature, relating the conductivity to the composition of the mixture, the classical relationship derived by Maxwell (1892) is mainly recommended as being reliable. Turner (1976), for example, demonstrated that the Maxwell relation can be used in fluidized beds up to the packed bed value of the dispersed phase volume fraction

Correspondence concerning this article should be addressed to U. Böhm.

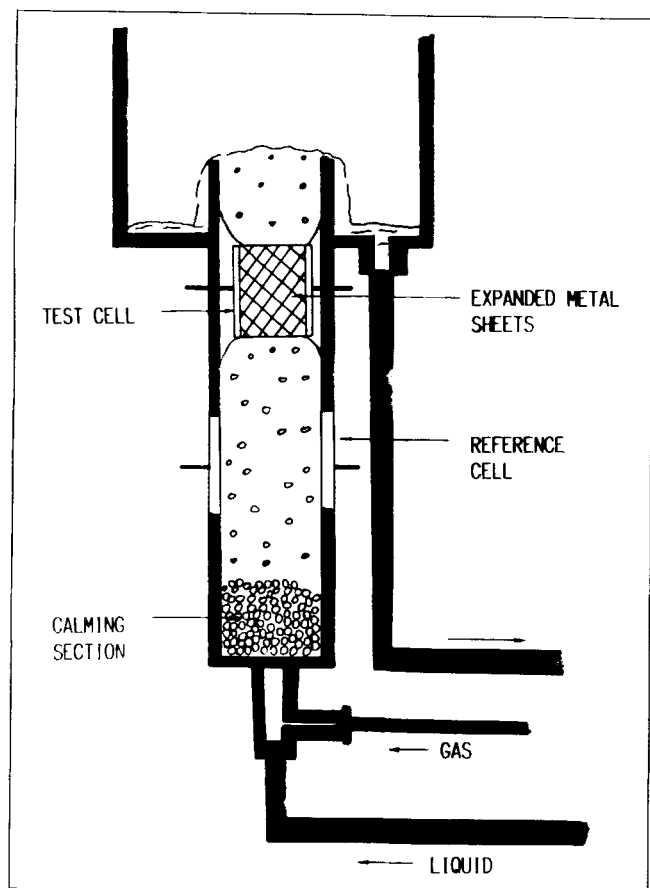


Figure 1. Experimental equipment.

and Sigrist (1978) showed experimentally that at gas void fractions up to 0.6 the conductivity of a gas-containing liquid can be calculated by the Maxwell equation. However, the presence of a metallic packing introduces a complication in the interpretation of the conductivity results.

In this work a model is developed which allows to apply the electrical conductivity technique for measuring the gas holdup in the presence of an expanded metal packing. Different arrays of stacked sheets are investigated, showing the influence of the geometry and the flow velocities on the gas void fraction.

Experimental

Figure 1 shows the experimental equipment. The column is made of lucite tube; its internal diameter is 5 cm and its total height, 60 cm. The lower part of the column contains glass spheres (0.5 cm in diameter) up to a height of 10 cm and acts as a calming section. The following section (15 cm height) contains, flush to the wall, the electrodes which conform a first conductivity cell, that will be called further on the "reference cell." This cell is used to measure the conductivity of the solution or the gas dispersion prior to its entrance in the expanded metal packing section.

In the test section itself, the column cross-section changes from circular to square (3 cm x 3 cm). Two opposed walls of the square duct contain the electrodes of a second conductivity cell which will be called the "test cell." In this cell the packing

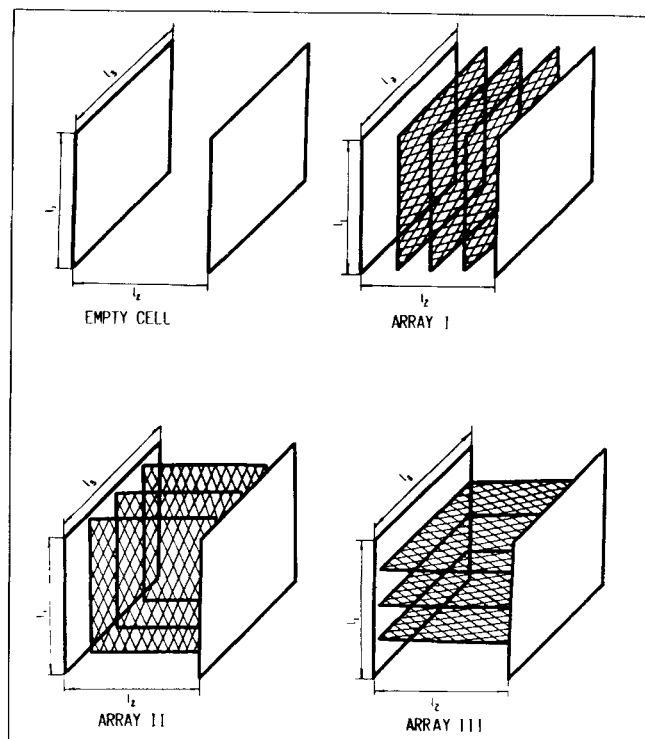


Figure 2. Sketch of test cell and expanded metal packings.

to be investigated is placed. The packing is built by stacking square sheets of expanded metal (EMS) thus forming a cube which fills completely the test cell. The commercial designation of the expanded metal is LD-N-E = 1.0-0.95-0.4, which means that the large diagonal of the rhombus is 1.0 cm long and the dimensions of the rib are 0.95 mm and 0.4 mm, respectively. 29 sheets were required to fill the cubic test cell.

The sheets can be stacked so that they remain parallel to the flow (Figure 2, arrays I and II) or perpendicular to the flow (Figure 2, array III).

Besides, in the first case, the sheets (parallel to the flow) can be placed either parallel or perpendicular to the electrodes of the test cell (Figure 2, arrays I and II) and every sheet can be oriented so that the large diagonal D or the small diagonal d of the rhombus of the expanded metal is in the flow direction (Figure 2, arrays II and I). For this investigation the three geometries shown in Figure 2 were selected among all possible combinations.

In order to avoid the electric short circuit between the electrodes of the conductivity cell and the EMS, the edges of the latter were coated with an insulating epoxy paint.

Finally, the upper part of the column has a 20 cm diameter vessel for disengaging the gas from the liquid. The liquid recirculates to a reservoir where it is maintained at $25 \pm 0.1^\circ\text{C}$.

The liquid is a potassium chloride solution, ca. 0.0125N. Its electric conductivity k_o is determined in each experiment with the help of a standard conductivity cell and with the reference cell. The gas is nitrogen, previously humidified. Both the liquid and the gas flow rates are measured with rotameters.

The conductance of both the reference and the test cell is determined for a given liquid flow rate and different gas flow

rates, beginning with single phase liquid flow. The measurements are repeated for other liquid flow rates, scanning the $0\text{--}130\text{ cm}^3\cdot\text{s}^{-1}$ range for both the liquid and the gas.

In the reference cell Maxwell's equation,

$$\frac{k}{k_o} = \frac{\rho_o}{\rho} = \frac{1 - \epsilon}{1 + \epsilon/2} \quad (1)$$

which relates the conductivity of the dispersion to its gas fraction, is directly applicable. On the other hand, the presence of metallic parts within the test cell makes it necessary to derive appropriate equations for obtaining the conductivity of the fluid phase from the conductance measurements.

Electrical Conductivity Model for the Packed Test Cell

To analyze the electrical conductance of a system composed by two parallel plane electrodes and between them N EMS electrically insulated from the electrodes, all immersed in an aqueous electrolyte, (0.0125 N KCl), a model has been developed which is described here. The conductance of the system will be a function of the electrical properties of the two phases as well as of the geometrical array of the EMSs. It is assumed that the electrical field is confined to a parallelepiped formed by the eight vertices of the two planar electrodes (Figure 2). End effects are neglected in view of the size of the electrodes, so that the electrical field lines are assumed to be straight and parallel.

Cell without packing

The electrical conductivity of the electrolyte has been obtained from the conductance measured with the test cell filled only with the electrolyte and applying the geometrical factor $l_2/l_1 \cdot l_3$. This result agrees within 1% with the conductivity obtained with a standard cell. This difference of 1%, due to the end effects, will be considered further on as the systematic error of the model.

From impedance measurements of the test cell at different angular frequencies (Figure 3a) it is inferred that at frequencies larger than 1.5 kHz the behavior of the cell tends to that of an ideal system and an equivalent circuit as shown in Figure 3b results. C_o is the double layer capacitance of each interface and R_o is the electrolyte resistance and the following equation holds for the circuit:

$$Z(\omega) = R_o + 2/(j\omega C_o) \quad j = \sqrt{-1} \quad (2)$$

and

$$\lim_{\omega \rightarrow \infty} Z = R_o = 1/G_o \quad (3)$$

where

$$R_o = \rho_o \frac{l_2}{l_1 l_3} \quad (4)$$

In the present case Eq. 3 strictly applies for frequencies of 25 kHz and larger.

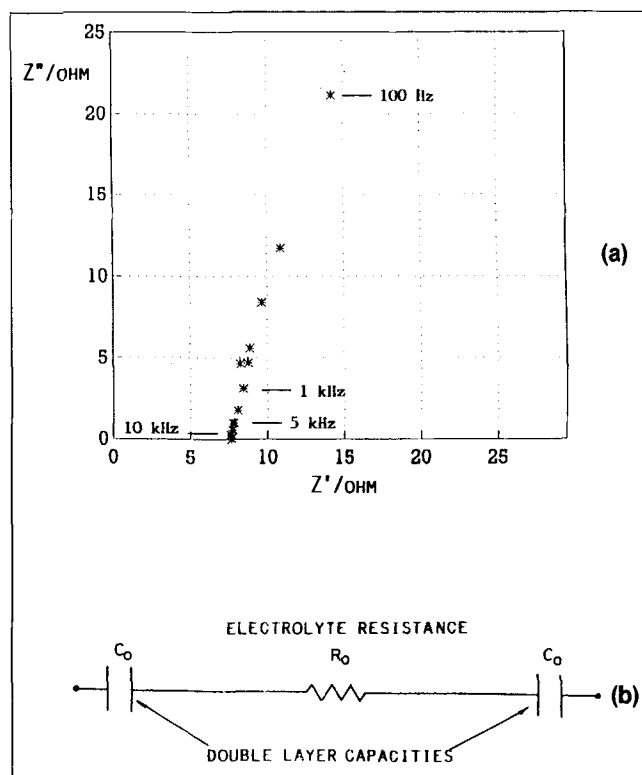


Figure 3. (a) Nyquist diagram for test cell without packing; KCl 0.26 N, $T = 298.6\text{ K}$; (b) equivalent circuit of test cell without packing.

Array I

The EMSs stand parallel to the electrodes, so that their rhombic openings allow to form p liquid branches across them. Each branch can be described by an equivalent circuit similar to that of Figure 3b and Figure 4a. The remaining cell space is occupied by alternating layers of liquid (C_v', R_v', C_v''), EMS material (C_v'', R_m, C_v'), liquid (C_v'', R_v', C_v'), and so on. The equivalent circuit is shown in Figure 4b.

The p circuits shown in Figure 4a as well as the one shown in Figure 4b are connected in parallel, since their terminals "A" and "B" are at the same potential, Figure 4c.

The impedance of this equivalent circuit results:

$$\frac{1}{Z} = \frac{p}{R_v + 2/(j\omega C_v)} + \left[\frac{2N}{j\omega C_v''} + \frac{2}{j\omega C_v'} + N R_m + (N+1) R_v' \right]^{-1} \quad (5)$$

N is the number of EMS that fill the space between the electrodes. The thickness of each EMS is assumed to be equal to the thickness of each liquid layer between them; therefore a value of $l_2/(2N+1)$ is obtained for both of them (l_2 = total cell width, Figure 2).

The cross-sectional area of the metallic (EMS) phase is given by the difference between the total cell area $A = l_1 \cdot l_3$ and the area of the p liquid branches $p \cdot A_b$.

Therefore the expressions for the circuit resistances are the following:

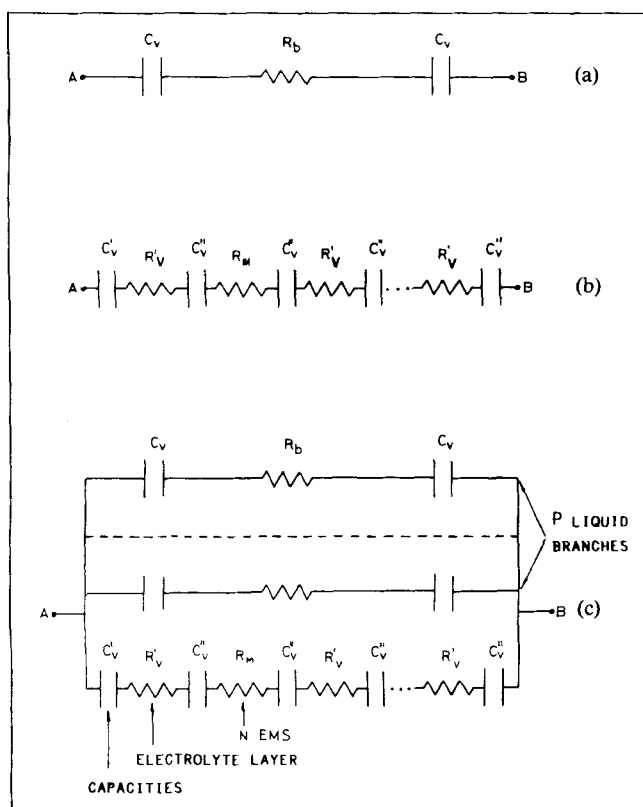


Figure 4. Equivalent circuits for array I.

(a) liquid branch; (b) electrode, alternating layers of liquid, EMS, liquid, and so on; (c) whole packing.

$$R_M = \rho_M \frac{l_2}{2N+1} \frac{1}{A-pA_b} \quad (6)$$

$$R'_v = \rho_o \frac{l_2}{2N+1} \frac{1}{A-pA_b} \quad (7)$$

$$R_b = \rho_o \frac{l_2}{A_b} \quad (8)$$

and

$$A_b = \frac{d \cdot D}{2} \quad (9)$$

where D and d are the large and small diagonals of the rhombus.

From Eq. 5 it can be shown that

$$\lim_{w \rightarrow \infty} Z = \frac{R_b [NR_M + (N+1)R'_v]}{p[NR_m + (N+1)R'_v] + R_b} \quad (10)$$

Since $\rho_M = 7.2 \cdot 10^{-5} \text{ ohm} \cdot \text{cm}$ for stainless steel (Weast, 1986) and $\rho_o = 365.9 \text{ ohm} \cdot \text{cm}$ for the 0.0125 N KCl solution as determined experimentally, from Eqs. 6 and 7 a ratio $R'_v/R_M = 5.1 \cdot 10^6$ results, and the expression Eq. 10 is reduced to

$$\lim_{w \rightarrow \infty} Z = \frac{R_b (N+1)R'_v}{p(N+1)R'_v + R_b} = 1/G_E \quad (11)$$

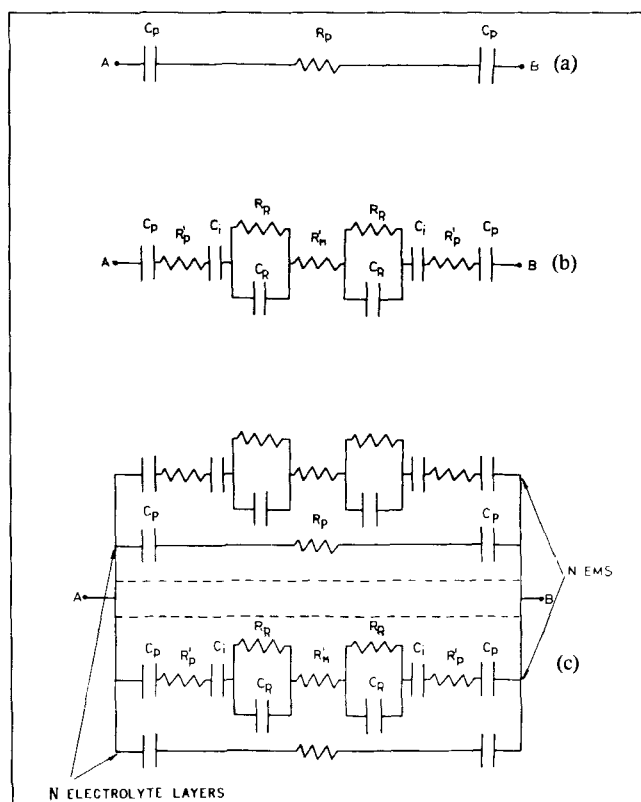


Figure 5. Equivalent circuits for arrays II and III.

(a) liquid layer; (b) expanded metal sheet-electrolyte; (c) whole packing.

Arrays II and III

In these configurations the EMSs are arranged either vertically (array II) or horizontally (array III), but in both cases perpendicular to the electrodes. The following model applies for both arrays.

In these geometries adjacent EMSs of thickness $l_3/2N$ in array II ($l_1/2N$ in array III) are separated by electrolyte layers of thickness $l_3/2N$ ($l_2/2N$).

The equivalent circuit of each electrolyte layer is shown in Figure 5a.

Due to the enormous difference between the resistivities of the metal and electrolyte, the EMS is considered as a continuous metallic plate with a resistance R'_M between the opposite edges of the EMS, thus neglecting the effect of the electrolyte that fills the rhombic openings of the EMS. The dimensions of this metallic plate are taken as an average between the maximal and minimal dimensions of the EMS (Figure 6).

The edges of the metallic plate are assumed to be coated with an insulating paint as in the real case. The equivalent circuit corresponding to each EMS is shown in Figure 5b. It contains a capacitance which represents the double layer at the electrode-electrolyte interface (C_p); the resistance of the electrolyte layer between the electrode and the edge of the EMS (R_p); a capacitance of the electrolyte-coating interface (C_i); the epoxy coating is represented by a very high resistance (R_R) in parallel with a capacitance (C_R); the resistance of the metallic plate (R'_M). Similar components are repeated in the vicinity of the opposed electrode. Since the terminals of both

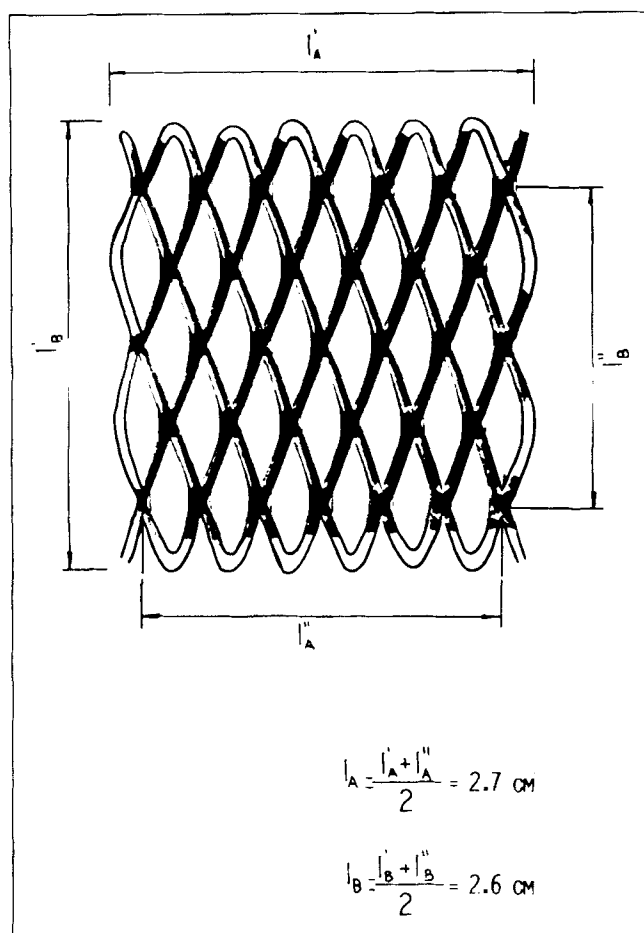


Figure 6. Expanded metal sheet.

equivalent circuits are at the respective electrode potentials, they are connected in parallel. Therefore the overall equivalent circuit involves N parallel connections of each type, Figure 5c.

The following equation has been derived for the impedance of this circuit:

$$\frac{1}{Z} = \frac{N}{R_p - \frac{2j}{C_p w}} + \frac{N}{(R_M' + 2R_p') - \frac{2j}{w} \left(\frac{1}{C_p} + \frac{1}{C_i} \right) + \frac{2R_R}{1 + jR_R C_R w}} \quad (12)$$

In the limit of high frequencies the expression for the impedance results:

$$\lim_{w \rightarrow \infty} Z = \frac{R_p(R_M' + 2R_p')}{(R_M' + 2R_p' + R_p)N} \quad (13)$$

where

$$R_p = \rho_o \cdot 2N l_2 / (l_1 l_3) \quad (\text{arrays II and III}) \quad (14)$$

Table 1

	Without EMS	Array I	Array II	Array III
$\rho_o / \text{ohm} \cdot \text{cm}^{-1}$	365.9	362.7	368.1	397.9
$G_E (\text{exp.}) / \text{mS}$	8.20	10.66	45.47	29.61
$G_E (\text{calc.}) / \text{mS}$	8.19	10.81	44.84	29.72
Relative error	-0.1%	1.4%	-1.4%	0.4%

$$R_p' = \rho_o \cdot (l_2 - l_A)N / (l_1 l_3) \quad (\text{array II}) \quad (15)$$

$$R_p' = \rho_o \cdot (l_2 - l_B)N / (l_1 l_3) \quad (\text{array III}) \quad (15(a))$$

R_M' was determined experimentally yielding

$$R_M' = 8.8 \cdot 10^{-3} \text{ ohms} \quad (\text{arrays II and III})$$

Taking into account that R_M' is 10^5 times smaller than R_p or R_p' , Eq. 13 reduces to

$$\lim_{w \rightarrow \infty} Z = 2R_p R_p' / [N(R_p + 2R_p')] = 1/G_E \quad (16)$$

It should be pointed out that in Eq. 16 the dependence of Z_{eq} on the number N of EMSs cancels out owing to the functionality of R_p and R_p' with N , Eqs. 14 and 15.

It can be concluded that the equivalent cell conductance G_E (Eqs. 11 and 16) in every case depends on the resistivity of the electrolyte and on a geometrical factor. The geometrical factor is a function of the dimensions of the EMS and in the case of array I of the number N of EMSs.

Results and Discussion

Single phase flow

To confirm the validity of the electrical conductivity model, experiments were carried out with the electrolyte alone, flowing either through the empty test cell or through the test cell containing the expanded metal packing. Since the electrolyte concentration registered slight variations from run to run, the electrolyte resistivity was determined directly for each run by measuring the conductance in the reference cell, whose cell constant is $1/s = 0.201 \text{ cm}^{-1}$.

Table 1 summarizes the experimental values of electrolyte resistivity and of cell conductance and the calculated results using Eqs. 3, 11 or 16.

The agreement is highly satisfactory for the three arrays, bearing in mind the marked geometrical differences between them, which yield very different conductances.

The maximum relative error is 1.4%.

Two-phase flow

As stated before, the conductance of the reference cell and of the test cell with the different arrays was measured for liquid-gas dispersions flowing through them. Applying now Eqs. 3, 11 or 16 the electric resistivity of the dispersion, ρ , can be deduced and with the help of Maxwell's equation the gas holdup is obtained.

Figures 7 and 8 show the results of the gas holdup as a function of the gas superficial velocity, for the different liquid flow rates tested.

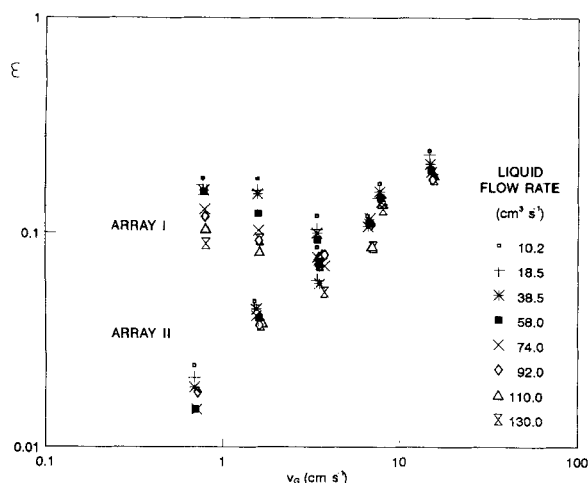


Figure 7. Gas holdup in arrays I and II as function of gas superficial velocity.

From Figure 8 it is evident that in the reference cell, with no packing, the gas fraction is roughly proportional to the gas velocity. In the light of the scattering in the data, due to the error of the experimental method, it can be deduced that the gas holdup is insensitive to the liquid velocity within the experimental range.

In the test cell, which holds the expanded metal packing arrays I, II and III a strong dependence of the gas holdup on the geometry of the packing itself is observed.

In the array II with the expanded metal sheets and their large dimension oriented in the flow direction, no additional gas retention is observed with respect to the reference cell; its behavior is similar to that of an empty bubble column.

The arrays I and III exhibit a considerable increase in the gas fraction at low gas velocities when compared with the reference cell. At these low gas flow rates the gas holdup diminishes systematically with increasing liquid velocity. At higher gas velocities the gas accumulation is reduced, and simultaneously the effect of the liquid velocity is not so marked. In other words, at higher gas velocities the systems tend to behave like the reference cell.

The geometrical configuration of these arrays, I and III, is much more compact in the direction of the flow, thus allowing the accumulation of stagnant bubbles.

Other authors (Leroux and Coeuret, 1983 and 1985), while studying the mass transfer in similar systems, observed higher transfer rates in arrays with horizontal sheets (like III) and arrays with the small dimension in the flow direction (array I). Considered from a fluid dynamic point of view, these geometries are better turbulence promoters and the eddies generated retain the bubbles.

Figure 9 illustrates the behavior of the different arrays as compared with the empty column, for a given liquid flow rate. At low gas velocities the gas fraction in the packed column can be as high as 17 times the value of the empty column (arrays I and III). Instead, this variation is not observed in array II.

This means that, when increases in the gas fraction are required (as may be the case in chemical reactors) or, on the contrary, the rapid elimination of the gas bubbles is sought

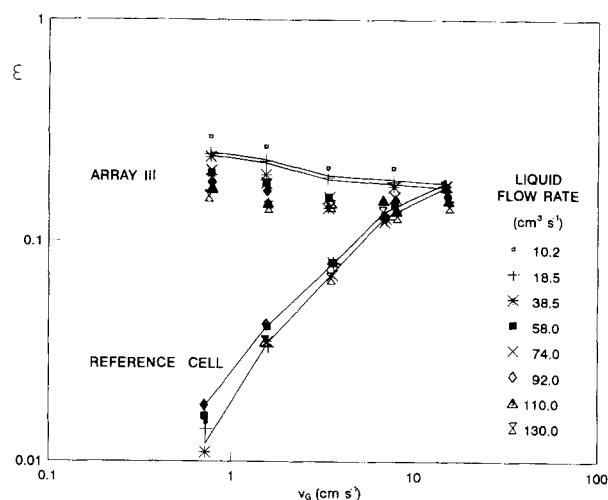


Figure 8. Gas holdup in array III and reference cell as function of gas superficial velocity.

The graph of errors shown corresponds to ϵ values obtained with $18.5 \text{ cm}^3 \cdot \text{s}^{-1}$ of liquid flow rate in array III and to mean values in the reference cell.

(as in electrochemical reactors) the proper choice of the packing array can be made accordingly.

It should be emphasized that arrays II and III are totally equivalent regarding their conductimetric behavior. This is verified in the measurements on the pure liquid phase. However, it is the model itself which allows detection of the different behavior of these packings in the presence of the gas phase.

Conclusions

A theoretical model has been developed, which predicts the conductivity behavior in the presence of a metallic expanded sheet packing in the cell.

The validity of this model has been verified with single phase flow.

The conductivity model applied to a gaseous dispersion flowing through the packing of the EMS allows the determination of the gas holdup.

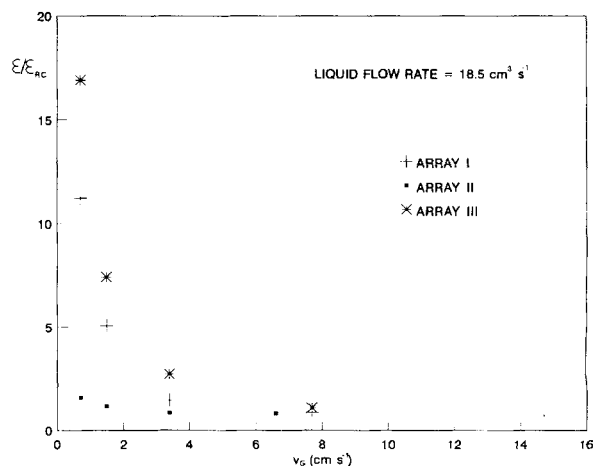


Figure 9. Gas holdup of different arrays as compared to the reference cell.

In the absence of packing, the gas fraction is not influenced by the liquid velocity. When the packing is introduced for a given gas flow rate the gas fraction may diminish with increasing liquid velocity, depending on the geometry of the array. The gas holdup in the packing reduces at high gas velocities.

There is a strong dependence of the gas holdup with the orientation of the sheets and of the large dimension of the expanded metal with respect to the flow direction.

At low gas velocities the gas fraction in the packed column can be up to as 1,700% larger than the gas fraction of the entering dispersion.

Notation

A = cell area, cm^2
 A_b = liquid branch area, cm^2
 C_i = interfacial capacitance (electrolyte-epoxy coating, arrays II and III), F
 C_o = double layer capacitance, F
 C_p = double layer capacitance (electrode-electrolyte layer, arrays II and III), F
 C_R = capacitance of epoxy-coating, F
 C_v = double layer capacitance, F (electrode-liquid branch, array I)
 C_v' = double layer capacitance, F (electrode-liquid layer, array I)
 C_v'' = capacitance, F (EMS-liquid layer, array I)
 d = small diagonal of rhombus, cm
 D = large diagonal of rhombus, cm
 f = frequency, Hz
 G_o = conductance of empty test cell, Ω^{-1}
 G_E = conductance of cell with packing, Ω^{-1}
 k = conductivity of gas-liquid dispersion, $\Omega^{-1} \cdot \text{cm}$
 k_o = conductivity of continuous phase, $\Omega^{-1} \cdot \text{cm}$
 l_A = characteristic length of sheet (Figure 6)
 l_B = characteristic length of sheet (Figure 6)
 l_1 = height of electrodes, cm
 l_2 = distance between electrodes, cm
 l_3 = width of electrodes, cm
 N = number of EMS
 p = number of liquid branches
 R_b = liquid branch resistance, Ω
 R_M = EMS resistance, Ω
 R_o = electrolyte resistance, Ω
 R_p = resistance of electrolyte layers (arrays II and III)
 R_R = resistance of epoxicoating, Ω
 R_M' = resistance between opposite edges of EMS, Ω
 R_p' = resistance of liquid layer (electrode-EMS edge arrays II and III), Ω

R_v' = liquid layer resistance (array I), Ω
 v_G = gas superficial velocity, $\text{cm} \cdot \text{s}^{-1}$
 ω = angular frequency = $2 \pi \cdot f$, $\text{rad} \cdot \text{s}^{-1}$
 Z = impedance, Ω

Greek letters

ϵ = gas holdup
 ϵ_{RC} = gas holdup in reference cell
 ρ = resistivity of dispersion (gas-liquid), $\Omega \cdot \text{cm}^{-1}$
 ρ_M = stainless steel resistivity, $\Omega \cdot \text{cm}^{-1}$
 ρ_o = electrolyte resistivity, $\Omega \cdot \text{cm}^{-1}$

Literature Cited

- Cavatorta, O. N., and U. Böhm, "Mass Transfer in Electrolytical Cells with Gas Stirring," *J. Appl. Electrochem.*, **17**, 340 (1987).
Cavatorta, O. N., U. Böhm, and A. M. Chiappori de del Giorgio, "Mass Transfer in Annular Electrolytic Cells with Gas Stirring," *J. Appl. Electrochem.*, **21**, 40 (1991).
Gianetto, A., and P. L. Silvestone, "Multiphase Chemical Reactors," Hemisphere Publishing Corporation, Washington, p. 432 (1986).
Kreysa, G., and H. Y. Küpfs, "A New Electrochemical Gas Purification Process," *Ger. Chem. Eng.*, **6**, 325 (1983).
Leroux, F., and F. Coeuret, "Mass Transfer and Potential Distribution within Axial Flow through Electrodes of Expanded Metal," *Electrochim. Acta*, **28**, 1857 (1983).
Leroux, F., and F. Coeuret, "Flow by Electrodes of Ordered Sheets of Expanded Metal. Mass Transfer and Current Distribution," *Electrochim. Acta*, **30**, 159 (1985).
Maxwell, J. C., *A Treatise on Electricity and Magnetism*, 3rd ed., Clarendon Press, Oxford, p. 440 (1892).
Meredith, R. E., and C. W. Tobias, "Conduction in Heterogeneous Systems," *Adv. Electrochem. Electrochem. Eng.*, **2**, 15 (1962).
Piovano, S., O. N. Cavatorta, and U. Böhm, "Mass Transfer to Planar and Expanded Metal Electrodes in Bubble Columns," *J. Appl. Electrochem.*, **18**, 128 (1988).
Sigrüst, L., "Verfahrenstechnische Aspekte von Elektrolysezellen mit stark gasenden Elektroden," Thesis No. 6286, ETH Zürich (1978).
Turner, J. C. R., "Two Phase Conductivity. The Electrical Conductance of Liquid-Fluidized Beds of Spheres," *Chem. Eng. Sci.*, **31**, 487 (1976).
Vogt, H., *A Comprehensive Treatise of Electrochemistry*, Vol. 6, J. O' M. Bockris, B. E. Conway, E. Yeager, and R. E. White, eds., Plenum, New York, p. 471 (1983).
Weast, R. C., *Handbook of Chemistry and Physics*, 67th edition, CRC Press, Boca Raton, p. D-184 (1986).

Manuscript received Sept. 23, 1991, and revision received June 20, 1992.